MEASUREMENTS OF THE MOMENTUM COMPACTION FACTOR OF THE ESRF STORAGE RING

N. Carmignani*, W. De Nolf, A. Franchi, Ch.J. Sahle, L. Torino, ESRF, Grenoble, France
B. Nash, Radiasoft LLC, Boulder, CO, USA

Abstract

In a storage ring, the momentum compaction factor can be obtained by measuring the variation of the beam energy as a function of the RF frequency. In this paper we present the measurement of the momentum compaction factor from two different methods. With the first, we measure the variation of the undulator spectra for different RF frequencies. With the second, we measure the variation of the hard x-rays flux produced by a dipole for different RF frequencies.

INTRODUCTION

Particles with different momenta in a storage ring will follow closed orbits with different lengths. The momentum compaction factor α_c is defined as

$$\alpha_c = \frac{\Delta L/L}{\Delta p/p}, \qquad (1)$$

where L is the length of the closed orbit and p is the momentum of the particle [1].

The period of the particle revolution τ depends on the momentum deviation, because of the change of closed orbit length and the change of the particle velocity, as

$$\frac{\Delta\tau}{\tau} = -\left(\frac{1}{\gamma^2} - \alpha_c\right)\frac{\Delta p}{p} = \eta_c\frac{\Delta p}{p}, \qquad (2)$$

where γ is the Lorentz factor and η_c is the slip factor. For high energy electron storage rings, the velocity change due to a change of momentum is negligible and $\eta_c = -\alpha_c$.

In a storage ring, the revolution period is defined by the frequency of the RF cavities. Equation 2 can be written as

$$\frac{\Delta f_{RF}}{f_{RF}} = -\alpha_c\frac{\Delta p}{p}. \qquad (3)$$

In order to measure α_c, the variation of beam energy as a function of the RF frequency can be measured.

There are different ways to measure the beam energy and the momentum compaction factor. One accurate method is to measure the spin depolarization [2, 3]. Some measurements and simulations have been performed at ESRF, but the depolarization resonance was found to be much broader than in other lower-energy synchrotron light sources and so the precision on the energy measurement was lower [4, 5].

This paper describes how to measure the variation of the beam energy and the momentum compaction factor in two ways:

- by measuring the undulator spectra [6];

- by measuring the hard x-rays flux from the dipole radiation.

_____
* nicola.carmignani@esrf.fr

ENERGY FROM UNDULATOR SPECTRUM

The spectrum of the undulator radiation is peaked in some energies, given by the undulator period λ_u and the undulator parameter K. The wavelength of the radiation of the fundamental peak of the undulator spectrum is

$$\lambda_1(\theta) = \frac{\lambda_u}{2\gamma^2}\left(1 + \frac{K^2}{2} + (\gamma\theta)^2\right), \qquad (4)$$

where θ is the angle from the axis of the radiation cone and K is the undulator parameter, which is defined as

$$K = \frac{eB_0\lambda_u}{2\pi m_e c}, \qquad (5)$$

where e is the elementary charge, B_0 is the peak magnetic field of the undulator, m_e is the electron rest mass and c is the speed of light [7].

The energy of the fundamental peak of the undulator radiation is proportional to the square of the electron beam energy. By measuring the variation of undulator's peak energy for different RF frequencies, we can measure α_c.

An experiment to measure α_c with two ESRF undulator beamlines (ID20 and ID21) has been performed. ID20 is located in a high β_x and high dispersion straight section, ID21 is in a low β_x and low dispersion straight section (Fig. 1). The dispersion derivative, which comes from magnet misalignments, is higher in ID21 than in ID20. The position of the radiation cone at the end of the beamlines changes more with beam energy in ID21 (Fig. 2).
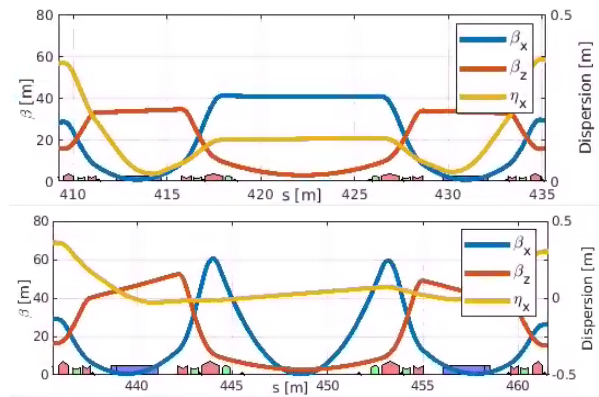

Figure 1: Linear optics from the orbit response matrix fit in the straight sections of ID 20 (top) and ID 21 (bottom).

The energy of the fundamental peak of the radiation produced by an undulator depends on the observation angle θ (Eq. 4): at large angle, the energy is lower. By selecting the

MC2: Photon Sources and Electron Accelerators

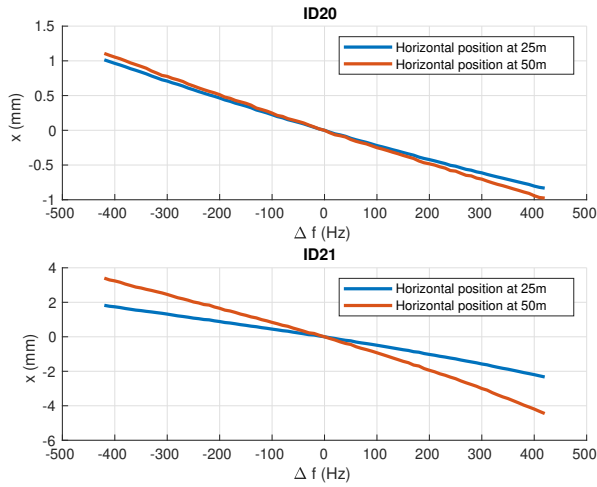A05 Synchrotron Radiation Facilities

Figure 2: Position of the x-ray beam as function of RF frequency change at 25 m and 50 m from the centre of ID20 and ID21 straight sections.

central part of the radiation cone, the energy distribution is sharper and centered on a higher value, as shown in Fig. 3.
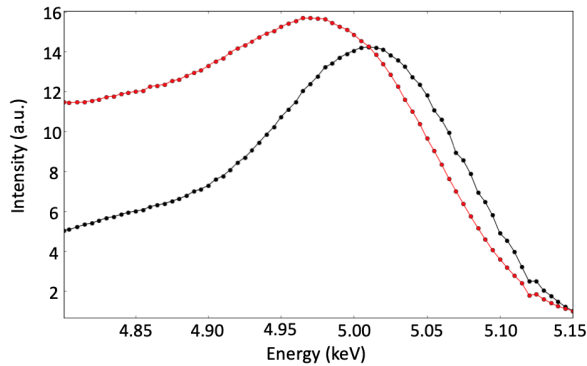

Figure 3: Spectrum of undulator of ID 21, with slits fully opened (red) at ± 2 mm horizontal and vertical and partially closed (black) at ± 0.05 mm.

The RF frequency has been scanned from $\Delta f = -400\,\text{Hz}$ ($\Delta E/E \simeq 0.64\%$) to $\Delta f = 300\,\text{Hz}$ ($\Delta E/E \simeq -0.48\%$).

At ID21, only the central part of the radiation cone has been selected using horizontal and vertical slits opened at ± 0.05 mm, because at large energy deviation the radiation cone was cut by the front-end aperture.

The undulator spectra are measured by measuring the x-ray flux with a fluorescent screen and a photodiode after the monochromator, scanning the monochromator angle. The peak is obtained by fitting a pseudo-Voigt distribution function to the measurement with SILX [8].

In both beamlines, a single undulator has been used for the experiment. In ID20, the gap aperture was 13.652 mm, which produces an x-ray beam with fundamental peak at 10 keV. In ID21, the gap aperture was 25.148 mm, which produces an x-ray beam with fundamental peak at 5 keV. The other undulators have been opened completely.

In Fig. 4, the plot of the variation of beam energy measured from the undulator radiation in ID20 and ID21 as a function of the RF frequency change is shown. From the linear component of the fit we can extract the value of α_c.
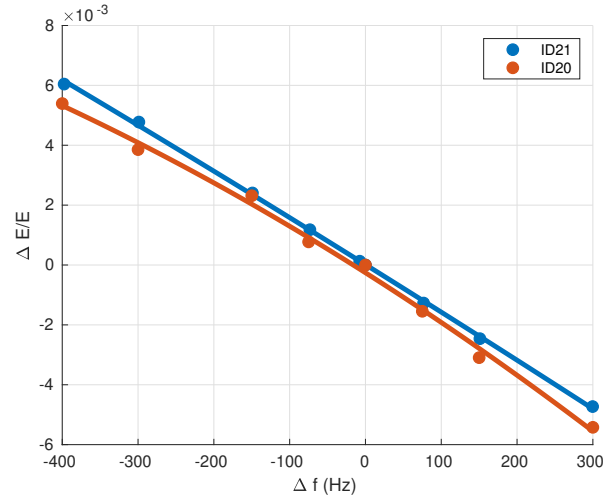

Figure 4: α_c measurement in ID20 and ID21 at ESRF.

The results of the measurements are reported in Table 1. The values are compatible with the α_c inferred from the model obtained by fitting the orbit response matrix (ORM) measured in the same day.

Table 1: Measurements of α_c in ID20 and ID21

ID	α_c (10^{-4})	α_c^{ORM} (10^{-4})
ID 20	1.77 ± 0.22	1.830 ± 0.004
ID 21	1.80 ± 0.04	

ENERGY FROM HARD X-RAY FLUX

The total power P emitted in synchrotron radiation by an electron in a bending magnet is given by

$$P = \frac{8}{3}\pi\varepsilon_0 r_0^2 c^3 \frac{E^2 B^2}{(mc^2)^2},\qquad(6)$$

where ε_0 is the vacuum permittivity, r_0 is the classical electron radius, E is the electron energy and B is the magnetic field [9].

The total power emitted depends on the electron beam energy, but it is difficult to measure. The intensity of the hard x-ray fraction (energies higher than 100 keV) of the synchrotron radiation depends strongly on the electron beam energy, as shown in Fig. 5, and it is easier to measure.

The hard x-rays are the only ones left after a few mm metal absorber. The variation of flux of these x-rays can be used to estimate the variation of the electron beam energy.

In Fig. 6, the experimental setup is described. In Fig. 7, an example of an image obtained by the CCD is shown.

A calibration factor between the variation of hard x-rays flux after the absorber ($\frac{\Delta I}{I}$) and the variation of beam energy has been simulated using the software XOP [10]. The

MC2: Photon Sources and Electron Accelerators
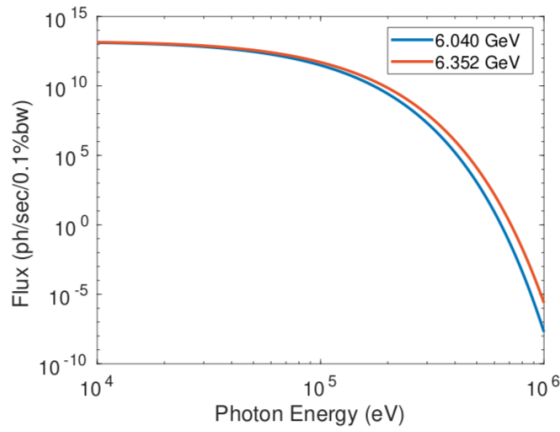
A05 Synchrotron Radiation Facilities

Figure 5: Simulated photon flux produced by a beam of 6.04 GeV (blue) and the one produced by increasing the beam energy of 5% (orange).
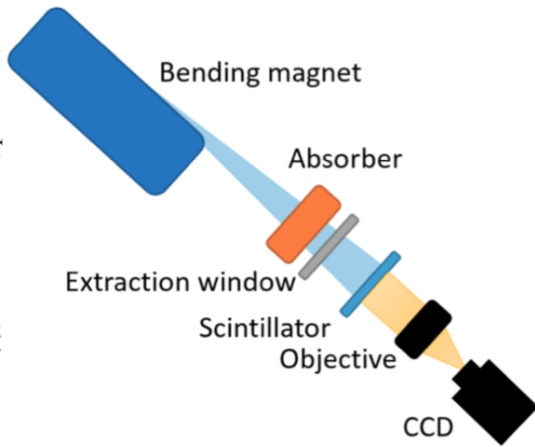

Figure 6: Experimental setup: the synchrotron radiation produced by a dipole is filtered by a copper absorber and extracted through an extraction window. The radiation is converted into visible light by a scintillator and imaged onto a CCD camera by an objective.

optical path model has been verified with a dedicated experiment, where the electron beam energy has been changed by changing the field of the dipoles [11]. The result is

$$\frac{\Delta I}{I} = 17.16 \cdot \frac{\Delta E}{E}. \qquad (7)$$

The measurement has been repeated three times, scanning the RF frequency in a small range of values, typically between $\Delta f = -40$ Hz and $\Delta f = +40$ Hz, with 1 Hz interval, and taking 10 measurements per frequency value. This procedure was possible because the measurement is very fast and it allowed to improve the precision of the result.

In Fig. 8 the result of a measurement is shown. In Table 2 three measurements performed in three different days are summarized.
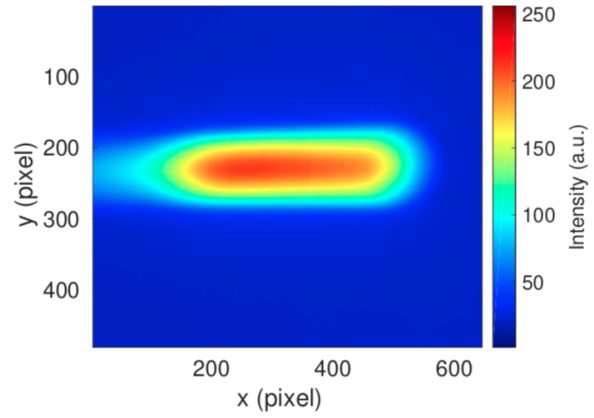
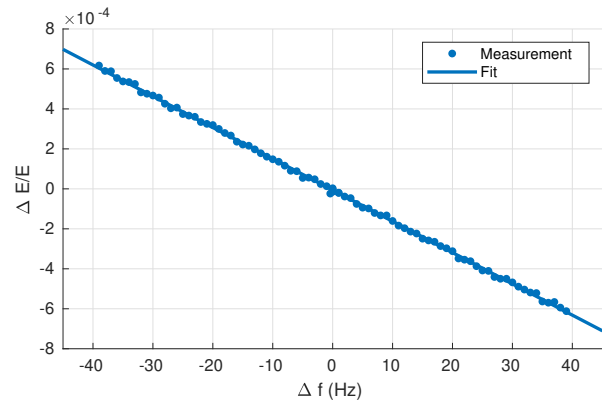Figure 7: Image obtained at the CCD camera.

Figure 8: $\Delta E/E$ dots are calculated from the SR intensity measurements, whereas the solid line represents the fit from whose slope the momentum compaction is inferred.

CONCLUSION

Using the undulator radiation, we could reach a precision on the measurement of α_c of about 2 % in ID 21, where only the central part of the radiation cone has been used. Using the hard x-ray flux from a dipole, the precision of the measurement was much higher, on 0.1 % level.

Two of the three measurements performed with the hard x-rays are about 1% smaller than the value of α_c of the accelerator model obtained by fitting the orbit response matrix measurements.

The use of the intensity of the synchrotron radiation to measure the energy variation has been proposed and could be used to monitor the beam energy oscillations.

Table 2: α_c Measurements Using Hard X-Ray Flux

Measurement #	α_c (10^{-4})	α_c^{ORM} (10^{-4})
1	1.814 ± 0.004	1.817 ± 0.004
2	1.816 ± 0.002	1.833 ± 0.004
3	1.806 ± 0.003	1.827 ± 0.004

REFERENCES

[1] H. Wiedemann, *Particle Accelerator Physics*, Springer, 2015.

[2] A.-S. Müller *et al.*, "Momentum Compaction Factor and Non-linear Dispersion at the ANKA Storage Ring", in *Proc. 9th European Particle Accelerator Conf. (EPAC'04)*, Lucerne, Switzerland, Jul. 2004, paper WEPLT068.

[3] K.P. Wootton *et al.*, "Storage ring lattice calibration using resonant spin depolarization", *Phys. Rev. Spec. Top. Accel. Beams*, vol. 16, p. 074001, 2013.

[4] J.-L. Revol *et al.*, "ESRF Operation Status", in *Proc. 9th Int. Particle Accelerator Conf. (IPAC'18)*, Vancouver, Canada, Apr.-May 2018, pp. 4088–4091. doi:10.18429/JACoW-IPAC2018-THPMF021

[5] N. Carmignani, F. Ewald, L. Farvacque, B. Nash, and P. Raimondi, "Modeling and Measurements of Spin Depolarization", in *Proc. 6th Int. Particle Accelerator Conf. (IPAC'15)*, Richmond, VA, USA, May 2015, pp. 109–112. doi:10.18429/JACoW-IPAC2015-MOPWA013

[6] E. Tarazona and P. Elleaume, "Measurement of the absolute energy and energy spread of the ESRF electron beam using undulator radiation", *Rev. Sci. Instr.*, vol. 67, no. 9, p. 3368, 1996. doi:10.1063/1.1147371

[7] H. Onuki and P. Elleaume, *Undulators, wigglers and their applications*, Taylor & Francis, 2003.

[8] ScIentific Library for eXperimentalists, https://zenodo.org/record/2592974#.XLbzeC-Q04U.

[9] A. Hofmann, "Characteristic of Synchrotron Radiation", Proc. CERN Accelerator School, Synchrotron Radiation and Free Electron Lasers, Chester, UK, Apr. 1989, pp. 115–141, published 1990, and CERN rep. CERN-90-03.

[10] X-Ray Oriented Program, www.esrf.eu/Instrumentation/software/data-analysis/xop2.4

[11] L. Torino, N. Carmignani, and A. Franchi, "Momentum Compaction Measurement Using Synchrotron Radiation", in *Proc. 7th International Beam Instrumentation Conference (IBIC'18)*, Shanghai, China, Sep. 2018, pp. 66–70. doi:10.18429/JACoW-IBIC2018-MOPA17